Supplementary Material

Atmospheric Aqueous Chemistry and Its Role in Secondary Organic Aerosol (SOA) Formation

Yong Bin Lim, Yi Tan, Mark J. Perri, Sybil P. Seitzinger, and Barbara J. Turpin

The supplementary material contains 10 pages with following information: Model development details; the chemical model (Table S1); the simulated concentration of dissolved oxygen during an experiment (Fig. S1); simulated tartaric acid shown with the ion abundances of m/z^- 149 and 103 (Fig. S2); and simulated malonic acid with the ion abundance of m/z^- 103.

The method of developing the model

1. Determining the rate constant for radical-radical reactions

The rate constants for the radical-O_2 reactions were set to be 1×10^6 $M^{-1}s^{-1}$ (Guzman et al., 2006). Since the reaction vessel contacts with the air, the Henry's law equilibrium for the O_2 is maintained in the gas and aqueous phase. In order to develop the kinetic model both the forward (the dissolution of O_2 in the air) and backward (the evaporation of dissolved O_2) rates have to be determined. For the rate of evaporation of dissolved O_2, the diffusion-controlled transfer coefficient value of 5.3×10^2 s^{-1} as suggested for cloud conditions (Warneck, 1999) was used. The rate of dissolution of O_2 was calculated by multiplying 1.3×10^{-3} (the Henry's law constant) by 5.3×10^2 s^{-1} (reaction 53 in Table S1). The rates for the radical-radical reactions were determined by fitting to the tartaric acid concentrations measured by IC. Note that the contribution of malonic acid to this peak appears to be minor (Fig. S2). In the model (Figure 3C) all C_4 dimers produced via radical-radical reactions are assumed to be tartaric acid because the model simulation indicates that tartaric acid formed from the reaction 12 in Table S1 accounts for ~ 80% of total C_4 dimers. It is possible that tartaric acid is formed through other C_4 dimer reactions as well (Reaction 18, 19, 20, 21, 23, and 28 in Table S1). The radical-radical reaction rate constant used is 1.3×10^9 $M^{-1}s^{-1}$ which is consistent with Guzman et al., (~ 2×10^9 $M^{-1}s^{-1}$) and Burchill et al. (1×10^9 $M^{-1}s^{-1}$).

2. Determining the dehydration/hydration rate constant for malonic acid formation by acid catalysis

Since malonic acid cannot be separately quantified by IC, the real-time profile of the ion abundance of *m/z*⁻ 103 obtained by ESI-MS was used. Here, we are not attempting to quantify malonic acid formation by the model, rather adjust the model parameters to fit the simulation to the ESI-MS real-time profile so we can obtain kinetic data for acid catalysis (Figure S3). Therefore, in Figure S3 the fit is made by normalizing the scales of ESI-MS signal intensity and simulated concentration. In the model, it is assumed that all C_3 dimers undergo dehydration and form malonic acid. Using the dehydration rate of 1×10^{-3} s^{-1} provides the best fit of simulated malonic acid (0-~50 minutes) to the m/z^- 103 profile. The decay of malonic acid (after ~50 minutes) has two contributors, hydration and OH radical reaction. It is impossible for the model to obtain a curve similar to the ESI-MS profile using rate constant of 3.0×10^8 $M^{-1}s^{-1}$ (Munger et al., 1995), which has been used for all OH radical reactions of C_3 dimers. Five different rate constants for the reaction of malonic acid + OH radicals are reported in Ervens et al. (2003). Only by using the lowest rate constant of 1.6×10^7 $M^{-1}s^{-1}$ (Walling and El-Taliawi, 1973) does simulated malonic acid have a shape similar to the ESI-MS profile. The simulation indicates that the upper limit for the hydration rate is 1×10^{-8} s^{-1}, which means that the major sink of malonic acid is OH radical reaction.

Supplementary Material References

Burchill, C. E. and Peron, K. M.: Radication-induced rearrangement of ethylene glycol in aqueous solution, Candadian J. Chem., 49, 2382-2389, 1971.

Carter, W. P. L., Darnall, K. R., Graham, R. A., Winer, A. M., and Pittts, Jr., J.: Reactions of C_2 and C_4 α–Hydroxy radicals with Oxygen, J. Phys. Chem., 83, 2305-2311, 1979.

Ervens, B., Gligorovski, S., and Herrmann, H.: Temperature-dependent rate constants for hydroxyl radical reactions with organic compounds in aqueous solutions, Phys. Chem. Chem. Phys., 5, 1811-1824, 2003.

Guzman, M. I., Colussi, A. J., and Hoffman, M. R.: Photoinduced oligomerization of aqueous pyruvic acid. J. Phys. Chem. A., 110, 3619-3626, 2006.

Lim, H. J., Carlton, A. G., and Turpin, B. J.: Isoprene forms secondary organic aerosol through cloud processing: model simulations, Environ. Sci. Tech., 39, 4441-4446, 2005.

Monod, A. and Doussin, J. F.: Structure-activity relationship for the estimation of OH-oxidation rate constants of aliphatic organic compounds in the aqueous phase: alkanes, alcohols, organic acids and bases, Atmos. Environ., 42, 7611-7622, 2008.

Munger, J. W., Jacob, D. J., Daube, B. C., Horowitz, L. W., Keene, W. C., and Heikes, B. C., J.: Formaldehyde, glyoxal, and methylglyoxal in air and cloudwater at a rural mountain site in central Virginia, Geophys. Res., 100(D5), 9325-9333, 1995.

Tan, Y., Perri, M. J., Seitzinger, S. P., and Turpin, B. J.: Effects of precursor concentration and acidic surfate in aqueous glyoxal-OH radical oxidation and implications for secondary organic aerosol, Environ. Sci. Technol, 43, 8105-8112, 2009.

Walling, C. and El-Taliawi, G. M.,: Fenton's reagent. II. Reactions of carbonyl compounds and .alpha.,.beta.-unsaturated acids, J. Am. Chem. Soc., 95, 844-847, 1973

Warneck P.: The relative importance of various pathways for the oxidation of sulfur dioxide and nitrogen dioxide in sunlit continental fair weather clouds, Phys. Chem. Chem. Phys., 1, 5471-5483, 1999.

Table S1. Reactions and rate/equilibrium constants used in the full kinetic model of glyoxal + OH

	Reactions	Rate constants (M^{1-n} s^{-1})	Ref
1	$H_2O_2 \rightarrow 2OH$	1.1e-4	T
2	$OH + H_2O_2 \rightarrow HO_2 + H_2O$	2.7e7	T
3	$HO_2 + H_2O_2 \rightarrow OH + H_2O + O_2$	3.7	T
4	$2HO_2 \rightarrow H_2O_2 + O_2$	8.3e5	T
5	$OH + HO_2 \rightarrow H_2O + O_2$	7.1e9	T
6	$GLY + OH \rightarrow GLY^* + H_2O$	1.1e9	T
7	$GLY^* + O_2 \rightarrow GLYOO^*$	1.0e6	G
8	$GLYOO^* \rightarrow GLYAC + HO_2$	5.0e1	C
9	$2GLYOO^* \rightarrow 2CHOHOH + 2CO_2 + O_2 + 2H_2O$	3.0e8	e
10	$CHOHOH + O_2 \rightarrow HCO_2H + HO_2$	5.0e6	e
11	$GLY^* + CHOHOH \rightarrow C3D$	1.3e9	G
12	$GLY^* + GLY^* \rightarrow TA$	1.3e9	G
13	$GLYAC + OH \rightarrow GLYAC^* + H_2O$	3.62e8	T
14	$GLYAC^* + O_2 \rightarrow GLYACOO^*$	1.0e6	G
15	$GLYACOO^* \rightarrow OXLAC + HO_2$	5.0e1	C
16	$2GLYACOO^* \rightarrow 2CO_2 + 2COOH$	3.0e8	e
17	$COOH + O_2 \rightarrow CO_2 + H_2$	5.0e6	e
18	$GLY^* + COOH \rightarrow C3D$	1.3e9	G
19	$GLYAC^* + CHOHOH \rightarrow C3D$	1.3e9	G
20	$GLYAC^* + CHOHOH \rightarrow C3D$	1.3e9	G
21	$2GLYAC^* \rightarrow C4D$	1.3e9	G
22	$GLYAC^- + OH \rightarrow GLYAC^{*-} + H_2O$	2.9e9	T
23	$GLYAC^* + GLY^* \rightarrow C4D$	1.3e9	G
24	$GLYAC^{*-} + GLY^* \rightarrow C4D$	1.3e9	G
25	$GLYAC^{*-} + GLYAC^* \rightarrow C4D$	1.3e9	G
26	$2GLYAC^{*-} \rightarrow C3D$	1.3e9	G
27	$GLYA^{*-} + COOH \rightarrow C3D$	1.3e9	G
28	$GLYAC^{*-} + CHOHOH \rightarrow C3D$	1.3e9	G
29	$GLYAC^{*-} + O_2 \rightarrow GLYACOO^{*-}$	1.0e6	G
30	$GLYACOO^{*-} \rightarrow OXLAC^- + HO_2$	1.0e2	e
31	$2GLYACOO^{*-} \rightarrow 2CO_2^- + 2COOH$	3.0e8	e
32	$OXLAC + OH \rightarrow COOH + CO_2 + 2H_2O$	1.4e6	T
33	$OXLAC^- + OH \rightarrow COOH + CO_2^- + 2H_2O$	2.0e7	T
34	$OXLAC^{2-} + OH \rightarrow COOH + CO_2^- + OH^-$	4.0e7	T
35	$H_2O \leftrightarrow H^+ + OH^-$	K_{eq} = 1.0e-14 k_r = 1.4e11	T
36	$HO_2 \leftrightarrow H^+ + O_2^-$	K_{eq} = 1.6e-5 k_r = 5.0e10	T
37	$GLYAC \leftrightarrow H^+ + GLYAC^-$	K_{eq} = 3.47e-4 k_r = 2.0e10	T
38	$OXLAC \leftrightarrow H^+ + OXLAC^-$	K_{eq} = 5.67e-2 k_r = 5.0e10	T
39	$OXLAC^- \leftrightarrow H^+ + OXLAC^{2-}$	K_{eq} = 5.42e-5 k_r = 5.0e10	T
40	$CO_2^- + O_2 \rightarrow O_2^- + CO_2$	2.4e9	T
41	$GLYAC + H_2O_2 \rightarrow HCO_2H + CO_2 + H_2O$	0.3	T
42	$HCO_2H + OH \rightarrow COOH + H_2O$	1.0e8	T

43	$HCO_2^- + OH \rightarrow CO_2^- + H_2O$	2.4e9	T
44	$HCO_2H \leftrightarrow H^+ + HCO_2^-$	K_{eq} = 1.77e-4 k_r = 5.0e10	T
45	$GLY + H_2O_2 \rightarrow HCO_2H + HCO_2H$	0	T
46	$OH + O_2^- \rightarrow OH^- + O_2$	1.0e10	T
47	$HCO_2^- + OH \rightarrow CO_2^- + H_2O$	1.0e7	T
48	$CO_2^- + O_2^- \rightarrow CO_2^{-2} + O_2$	6.5e8	T
49	$CO_3^- + HCO_3^- \rightarrow HCO_3^- + CO_2^-$	1.5e5	T
50	$CO_3^- + H_2O_2 \rightarrow HCO_3^- + HO_2$	8.0e5	T
51	$CO_2 \leftrightarrow H^+ + HCO_3^-$	K_{eq} = 4.3e-7 k_r = 5.6e4	T
52	$HCO_3^- \leftrightarrow H^+ + CO_3^{2-}$	K_{eq} = 4.69e-11 k_r = 5.0e10	T
53	$O_2\,(g) \leftrightarrow O2$	K_{eq} = 1.3e-3 k_r = 5.3e2	W
54	$CO_2\,(g) \leftrightarrow CO_2$	K_{eq} = 3.4e-2 k_r = 5.3e2	L
55	$C3D + OH \rightarrow C3D^* + H_2O$	3.0e8	e
56	$C3D^* + O_2 \rightarrow C3DOO^*$	1.0e6	e
57	$C3DOO^* \rightarrow X + HO_2$	5.0e1	C
58	C3DOO* → 2COOH + 2GLYAC	3.0e8	e
59	$C4D + OH \rightarrow C4D^* + H_2O$	1.1e8	E
60	$C4D^* + O_2 \rightarrow C4DOO^*$	1.0e6	G
61	$C4DOO^* \rightarrow Y + HO_2$	5.0e1	C
62	2C4DOO* → 2GLYAC	3.0e8	e
63	2CHOHOH → GLY	1.3e9	G
64	CHOHOH + COOH → GLYAC	1.3e9	G
65	2COOH → OXLAC	1.3e9	G
66	$CO_2^- + COOH \rightarrow OXLAC^-$	1.3e9	G
67	$2CO_2^- \rightarrow OXLAC^{2-}$	1.3e9	G
68	$C3D \leftrightarrow MA + H_2O$	K_{eq} = 1e5 k_r = 1e-8	T
69	$MA + OH \rightarrow C3D^* + H_2O$	1.6e7	E
70	$TA + OH \rightarrow C4D^* + H_2O$	3.1e8	M

* = radical For example, glyoxal* = glyoxal radical; OO* = peroxy radical, C4D = C_4 dimer, TA = tartaric acid, C3D = C_3 dimer; MA = malonic acid, GLY = glyoxal, GLYAC = glyoxylic acid, OXLAC = oxalic acid, n = n^{th} order; K_{eq} = the equilibrium constant (M), k_r = the reverse rate constant for corresponding K_{eq}., Thus, the forward rate constant can be calculated by $K_{eq} \times k_r$; (g) = in the gas phase; X, and Y = anonymous organic products

Reference (Ref)

T = Tan et al., EST, 2009
G = Guzman et al., JPCA, 2006
C = Carlter et al., JPC, 1979
E = Ervens et al., PCCP, 2003
M = Monod et al., AE, 2008
L = Lim et al.,EST, 2005
W = Warneck, PCCP, 1999
e = Estimation by fitting

Tan, Y., Perri, M. J., Seitzinger, S. P., and Turpin, B. J.: Effects of precursor concentration and acidic surfate in aqueous glyoxal-OH radical oxidation and implications for secondary organic aerosol, Environ. Sci. Technol, 43, 8105-8112, 2009.

Guzman, M. I., Colussi, A. J., and Hoffman, M. R.: Photoinduced oligomerization of aqueous pyruvic acid. J. Phys. Chem. A., 110, 3619-3626, 2006.

Carter, W. P. L., Darnall, K. R., Graham, R. A., Winer, A. M., and Pittts, Jr., J.: Reactions of C_2 and C_4 α–Hydroxy radicals with Oxygen, J. Phys. Chem., 83, 2305-2311, 1979.

Ervens, B., Gligorovski, S., and Herrmann, H.: Temperature-dependent rate constants for hydroxyl radical reactions with organic compounds in aqueous solutions, Phys. Chem. Chem. Phys., 5, 1811-1824, 2003.

Monod, A. and Doussin, J. F.: Structure-activity relationship for the estimation of OH-oxidation rate constants of aliphatic organic compounds in the aqueous phase: alkanes, alcohols, organic acids and bases, Atmos. Environ., 42, 7611-7622, 2008.

Lim, H. J., Carlton, A. G., and Turpin, B. J.: Isoprene forms secondary organic aerosol through cloud processing: model simulations, Environ. Sci. Tech., 39, 4441-4446, 2005.

Warneck P.: The relative importance of various pathways for the oxidation of sulfur dioxide and nitrogen dioxide in sunlit continental fair weather clouds, Phys. Chem. Chem. Phys., 1, 5471-5483, 1999.

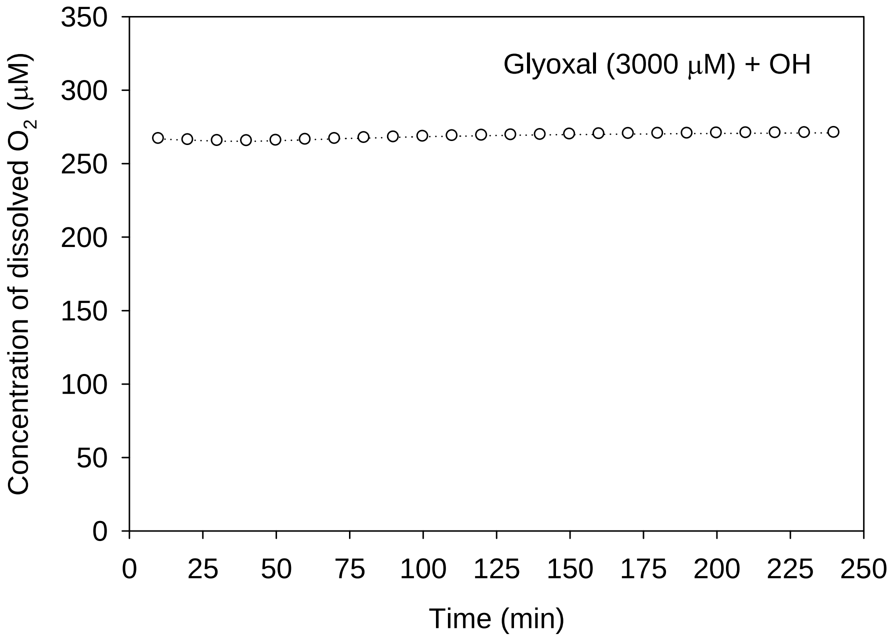

Fig. S1. The simulated concentration of dissolved O_2 during the reaction of glyoxal (3000 μM) + OH

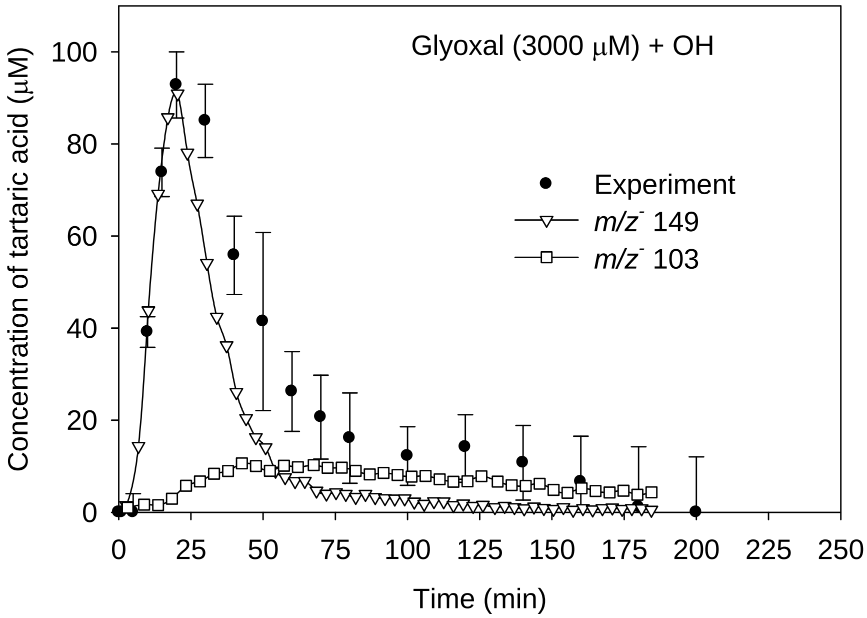

Fig. S2. The ESI-MS real-time profiles for *m/z*$^-$ 149 (tartaric acid) and *m/z*$^-$ 103 (malonic acid)

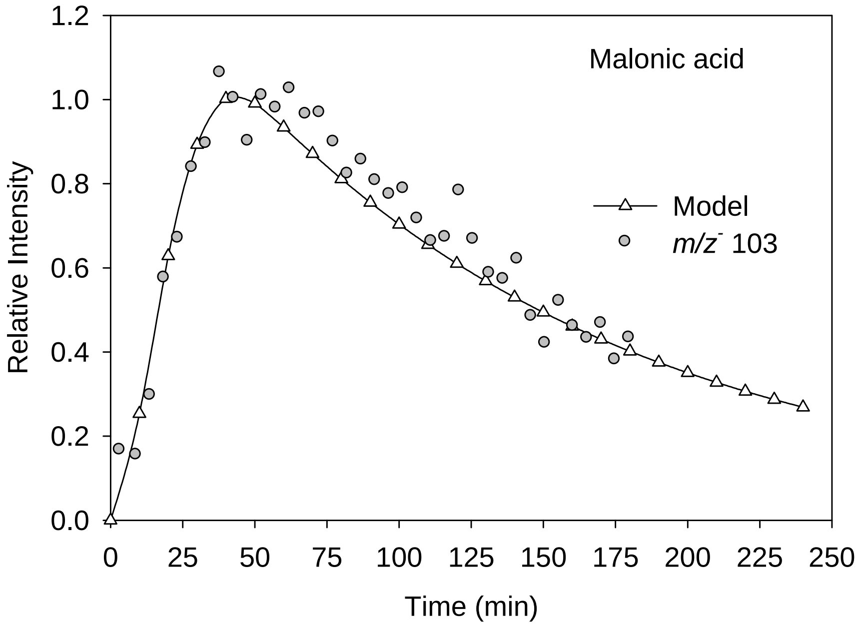

Fig. S3. The model simulation and the ESI-MS real-time profile for malonic acid